SEMARAK ILMU PUBLISHING

Journal of Advanced Research in Fluid Mechanics and Thermal Sciences

Journal homepage:
https://semarakilmu.com.my/journals/index.php/fluid_mechanics_thermal_sciences/index
ISSN: 2289-7879

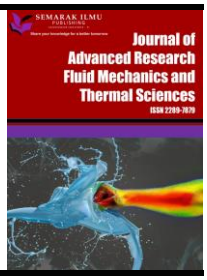

An Improvement in Boundary Treatment of Solid Boundary Using ISPH Approach

Nur'Ain Idris[1,*], Mitsuteru Asai[2], Hamidun Mohd Noh[3]

[1] Department of Civil Engineering, Centre for Diploma Studies, Universiti Tun Hussein Onn Malaysia, Pagoh Higher Education Hub, 84600 Pagoh, Johor, Malaysia
[2] Department of Civil Engineering, Kyushu University, 744 Motooka, Nishi-ku, Fukuoka 819-0395, Japan
[3] Department of Construction Management, Faculty of Technology Management and Business, Universiti Tun Hussein Onn Malaysia, 86400 Parit Raja, Johor, Malaysia

ARTICLE INFO

Article history:
Received 13 September 2022
Received in revised form 15 January 2023
Accepted 22 January 2023
Available online 13 February 2023

Keywords:
ISPH; boundary treatment; Neumann boundary condition; particle method

ABSTRACT

Incompressible Smoothed Particle Hydrodynamic (ISPH), one of the particle methods, is frequently employed to address a variety of challenging physical issues, such as those involving free surface flow. For measuring the precise and reliable pressure close to the boundary, the study of boundary treatment has lately been an active research field in the mesh-free or particle approach. If the solid barrier's appropriate pressure boundary condition is not met, fluid particles may penetrate it. This study proposes a straightforward boundary treatment that can satisfy the non-homogenous Neumann boundary condition on the solid boundary and the Dirichlet condition on the water surface. The main idea behind our suggested approach is that by solving a modified pressure Poisson equation, these boundary conditions are automatically satisfied. This technique can be improved such that it can be applied to any shape having a concave-convex boundary in addition to basic solid boundaries. The suggested method was tested using the hydrostatic case, followed by a numerical analysis validated using a 3D dam break flow with an opening gate and a Stanford rabbit demonstration. The outcome of the numerical modelling simulation was then contrasted with the findings of the theoretical and experimental studies. The obtained findings support the suggested technique by providing a good tendency and similarity output that enhances the boundary treatment on solid boundaries.

1. Introduction

Boundary conditions play an important role in numerical analysis, especially when involving two or more different types of boundaries. The issue of proper boundary treatment has received considerable critical attention from many researchers. Investigating it is a continuing concern to ensure the simulation gave precise and robust results, particularly at the boundary. Smoothed particle hydrodynamics (SPH) is a prevalent Lagrangian concept meshless particle method widely and actively used by researchers, especially in computational fluid dynamics nowadays. The SPH method

* *Corresponding author.*
E-mail address: ainidris@uthm.edu.my

https://doi.org/10.37934/arfmts.103.1.211222

was first developed by Lucy [1] and Gingold and Monaghan [2] about three decades ago, which originated from a simulation of astrophysical problematics. SPH method is a unique particle method that is meshless, does not require any grid, and has some advantages over the grid-based method, such as simplicity in implementation and ease of handling for larger deformations, even for complex fluid. Generally, there are two major groups of SPH for solving the viscous flow problem; the weakly compressible SPH (WCSPH), which solves an appropriate equation of state in fully explicit form and truly incompressible SPH (ISPH); it was extended to incompressible viscous flow [3]. Nowadays, a stabilized Incompressible Smoothed Particle Hydrodynamic (ISPH) approach is one of the particle methods and is frequently used to solve some difficult physical problems, including free surface flow problems.

There are many conventional methods of boundary treatment in the framework of SPH were introduced such as Fixed Wall Particle (FWP), Ghost boundary Particle (GBP) by Libersky and Petschek [4], Morris *et al.,* [5] and Yildiz *et al.,* [6]. Then, in 2011, Marrone *et al.,* [7] expanded the GBP to become Fixed Ghost Particles (FGP), and the improvement was made by Asai *et al.,* [8], introducing the Virtual Marker with Fixed Wall Particle (VMFWP), which includes the special treatment of slip and non-slip conditions with incompatible step-shape boundaries. The boundary treatment was continuously enhanced based on the literatures in the SPH framework. Despite being straightforward, the FWP method still has drawbacks that result in some particle penetration into the wall region across the computational domain. Then, by embedding the wall particles into the solid wall with a symmetrical point or mirrored image pairs, the GBP approach was proposed to address the shortcomings of the FWP method. Additionally, the method developed using FGP rather than conventional GBP improves homogeneity distribution and does not depend on the position of fluid particles, which lowers the computing cost because mirror particles are repositioned [7]. Idris and Sonoda [9] also have discussed detail on the boundary improvement which using the virtual marker of fixed wall particle. In addition, the dummy wall particles and analytical kernel renormalization wall boundary conditions are two different wall boundary conditions that have been explored by Nguyen *et al.,* [10] for the ISPH method. For the free-surface flow associated with solid-liquid phase change, Lan *et al.,* [11] enforced accurate wall boundary constraints to reduce velocity variations and compression near the solid wall. The boundary condition is not only focus in this area but also in the environmental wind profile area by Jena and Gairola [12].

Even though it is conceivable to have the homogeneous condition in the real condition, the homogenous Neumann boundary condition was nevertheless imposed from the aforementioned methods. Consequently, a modification known as a Modified Virtual Marker with Regular Grid will be discussed in this paper. By employing the suggested approach of boundary treatment, it will impose the non-homogenous Neumann boundary condition, meet the Dirichlet condition, and satisfy the actual condition, which in many situations has a value of pressure gradient. It has been verified and validated with hydrostatic compatible shape, dam break problem and bunny demonstration.

2. Methodology

2.1 Governing Equation

In this study, the basic stabilized ISPH was adopted, which was introduced by Asai *et al.,* [13]. The perception of ISPH included adjusting the source term in the treatment of pressure Poisson equation (PPE). In the following sections, the governing equations used and the concept of Smoothed Particle Hydrodynamics (SPH) with the modification for incompressible flow are described.

The continuity equation and the Navier-Stokes equation in the Lagrange description are given as follows

$$\frac{D\rho}{Dt} + \rho\nabla \cdot \mathbf{u} = 0 \tag{1}$$

$$\frac{D\mathbf{u}}{Dt} = -\frac{1}{\rho}\nabla p + v\nabla^2\boldsymbol{u} + \frac{1}{\rho^0}\nabla \cdot \tau + \mathbf{F} \tag{2}$$

whereby ρ and v are the density and kinematic viscosity of the fluid, u and p are the velocity vector and pressure of the fluid. Meanwhile, t indicates time, and F is an external force. The turbulence stress τ is necessary to denote the effects of the turbulence with coarse spatial grids. Generally, for the incompressible flow approach, the density is assumed by a constant value with its initial valueρ^0. Therefore, the governing equations lead to the following

$$\nabla \cdot \mathbf{u} = 0 \tag{3}$$

$$\frac{D_{\mathbf{u}}}{D_t} = -\frac{1}{\rho^0}\nabla p + v\nabla^2\mathbf{u} + \frac{1}{\rho^0}\nabla \cdot \tau + \mathbf{F} \tag{4}$$

2.2 Smoothed Particle Hydrodynamics (SPH) Approach

The basic concept of SPH is based on the interpolation method. The interpolation is based on the theory of integral interpolants by using kernels which approximate a delta function. A function at the sampling point can be expressed in integral form as follow

$$\phi(\boldsymbol{x}_i, t) = \int W(\boldsymbol{x}_i - \boldsymbol{x}_j, h)\phi(\boldsymbol{x}_j, t)dv = \int W(|\boldsymbol{x}_{ij}|, h)\phi(\boldsymbol{x}_j, t)dv, \tag{5}$$

where W is a weight function called a smoothing kernel function, as shown in Figure 1 and the subscript i and j indicate the positions of labeled particles.

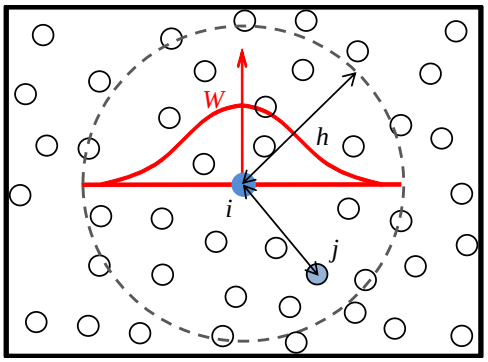

Fig. 1. Definition of smoothing length in the influence radius

In the smoothing kernel function, $|x_{ij}|=|x_i-x_j|$ and h are the distance between neighbor particles and the smoothing length. For the SPH numerical analysis, the integral equation in Eq. (5) is approximated by a summation of contribution from neighbor particles in the support domain as

$$\phi(\boldsymbol{x}_i, t) \approx \langle\phi_i\rangle = \sum_{j\in\mathbb{P}_i}\frac{m_j}{\rho_j}\phi_j W(|\boldsymbol{x}_{ij}|, h), \tag{6}$$

The ρ_j and m_j are the density and representative mass related to the particle j, respectively. The triangle bracket $\langle\phi\rangle$ means the SPH approximation of the function ϕ, and $\mathbb{P}_i$ is the asset of particle number related to particle i, as follows

$$\mathbb{P}_i \coloneqq \{j; h > |\boldsymbol{x}_{ij}|, j \neq i\} \tag{7}$$

2.3 Incompressible Smoothed Particle Hydrodynamics (ISPH) Approach

In general, the precision of the density representation in the SPH formulation and the handling of the pressure Poisson equation caused considerable difficulty in the SPH approach (PPE). The numerical density finds it challenging to maintain its starting value. In order to correct the ISPH's artificial pressure fluctuation error, the PPE is being re-examined in this instance.

The divergence-free condition was initially put forth by Cummins and Rudman [14] in the projection-based ISPH; Lee *et al.,* [15] extended it to the Reynolds turbulent model that included temporal averaging. Since the initial density of each particle is consistently assumed, it was referred to as a "really" incompressible algorithm, or ISPH. The PPE can then be approximated using SPH as follows;

$$< \nabla^2 p_i^{n+1} > = \frac{\rho^0}{\Delta t} < \nabla \cdot \mathbf{u}_i^* > \tag{8}$$

The particle density is updated on the intermediate particle positions in this density invariance system, and the particle position updates after each predictor step. The intermediate step's particle velocity is updated in the correction step using the pressure term. The final PPE form in ISPH can, therefore, roughly be redefined by the following;

$$< \nabla^2 p_i^{n+1} > = \frac{\rho^0 - \langle \rho_i \rangle}{\Delta t^2} \tag{9}$$

2.3 Pressure Dirichlet and Neumann Condition
2.3.1 Pseudo Neumann boundary condition: Dirichlet conditions

Using a similar approach as introduced by Asai *et al.,* [8], the external force and the pressure on each virtual marker will be estimated using the physical quantity in the particle's neighbourhood as shown in Eq. (6) with the normalized weight function. The pressure on the wall's particles in the border processing technique is not calculated by solving the modified pressure Poisson equation. Hence, the introduction of the solution of the PPE will give a whole boundary of Dirichlet condition, as shown in Figure 2, whereby approximation of the value of the wall particles pressure by denoting the value of the virtual marker to satisfy the Neumann boundary condition (Eq. (8)). The Dirichlet boundary causes the zero pressure of the particles of the free surface boundary conditions, which is marked with the red particles in Figure 2. In addition, since the coefficient matrix of the Poisson equation remains symmetric matrix needs not be modified, the solver of the simultaneous linear equations conjugates the gradient method using a diagonal scaling pre-processing (CG) method was used.

$$p'_w = \langle p_v \rangle + 2dp \langle \boldsymbol{f}_v \rangle . \boldsymbol{n} \tag{10}$$

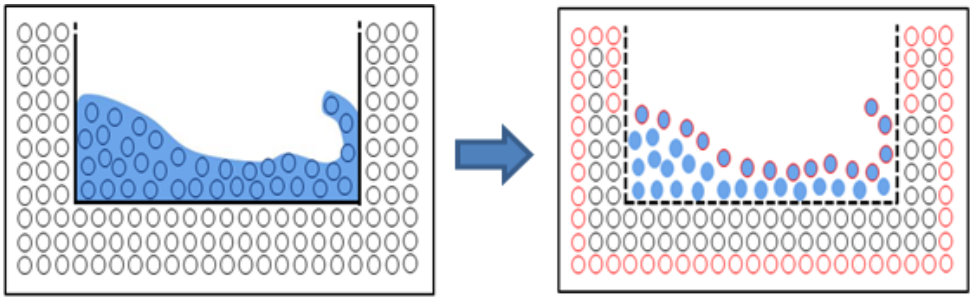

Fig. 2. Dirichlet conditions: Pseudo Neumann boundary condition

In this approach, the position of the virtual marker is proposed, as shown in the following equation, by locating the wall particles on the structured grid, the position of the virtual marker X ' using the distance d to the normal vector n. In this case, if n is defined at the global coordinate system, it is possible to create a virtual marker in the same procedure even in the non-conforming boundaries that do not match the actual smooth boundary. The location of the virtual marker identified as red X is depicted in Figure 3.

$$X' = \boldsymbol{X} + 2d\boldsymbol{n} \tag{11}$$

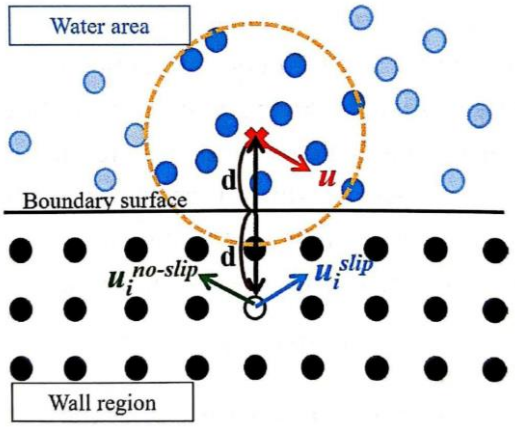

Fig. 3. Location of the virtual marker for slip and no-slip boundary velocity field using Pseudo Neumann boundary condition

2.3.1 Neumann boundary treatment (completely satisfies the pressure Neumann conditions)

In this section, the Modified Virtual Marker with Regular Grid (MVMRG), as a new boundary treatment that satisfies the non-homogenous Neumann boundary condition, will be described as a treatment to ensure a wall particle with precise physical properties, velocity and pressure. As a concern, solving PPE by giving the entire circumference Dirichlet condition zero pressure led to a lower pressure value than the actual hydrostatic pressure distribution in the district of wall particles. Therefore, the MVMRG is proposed to overcome this problem and attempt to strictly sufficient the non-homogenous Neumann boundary conditions.

The procedures will be briefly described; first, the wall particles placed similarly as in the Pseudo Neumann condition method defined in the previous section, placed equally spaced structural grid-like inside solid. Then, the location of the virtual markers on the boundary surface is no longer in the fluid area. Thus, by placing the wall particles on a structured grid, the X' position of the virtual markers

in the method uses the distance d to the normal vector n, and the boundary on the actual physical interface can be seen in Figure 4 and Figure 5.

$$\boldsymbol{X'} = \boldsymbol{X} + d\boldsymbol{n} \tag{12}$$

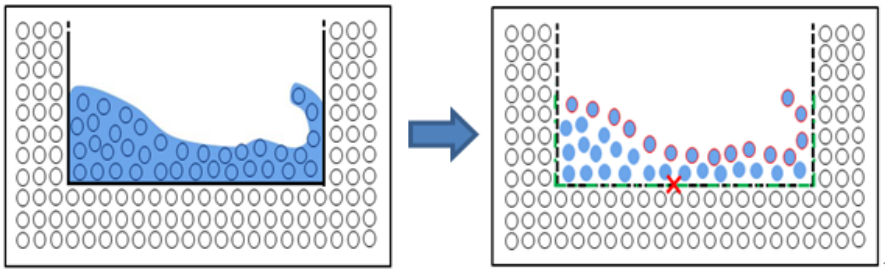

Fig. 4. Neumann boundary treatment

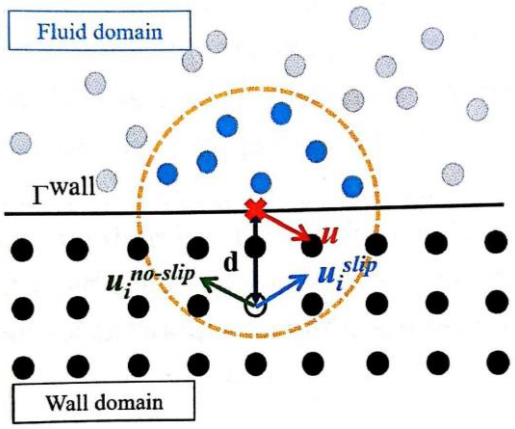

Fig. 5. Location of the virtual marker for slip and no-slip boundary velocity field using Neumann boundary condition

3. Results

3.1 Verification with Hydrostatic Tank

This section evaluates the hydrostatic pressure to investigate the effects of the boundary treatment used. The test was conducted by measuring the pressure near the bottom of the tank. This verification test is important to show the robustness and significance of the proposed boundary treatment. The tank was filled with a water height of 0.2m and 0.01m of particle size. The pressure measurement point is located in the middle bottom of the incompatible surface tank, as shown in Figure 6. The different outcomes on the contour pressure distribution, especially the effects near the side and bottom tank obtained using different treatments. It shows that the high-pressure distribution indicated using the proposed modified treatment, fully Neumann boundary condition, compared with the Pseudo Neumann boundary condition that shows a much lower pressure distribution, as depicted in Figure 7. Then, the numerical simulation result of the hydrostatic pressure was compared with the theoretical value of the hydrostatic pressure, as revealed in Figure 8.

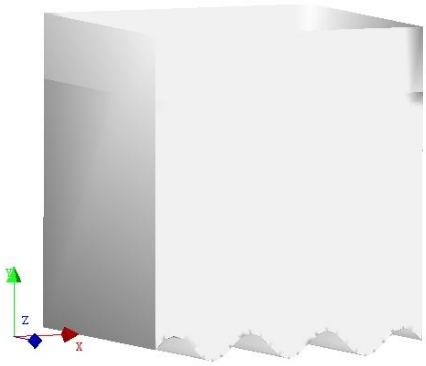

Fig. 6. Hydrostatic pressure for incompatible surface

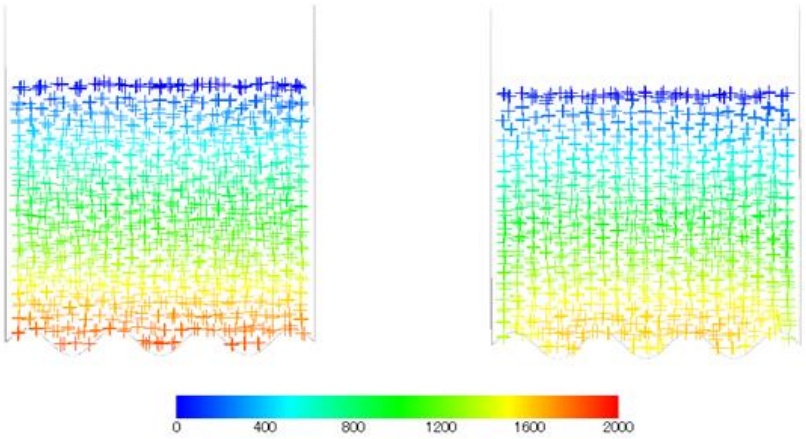

(a) (b)

Fig. 7. Distribution of pressure on the water particles using fully satisfied (a) Neuman boundary condition and (b) Pseudo Neumann boundary condition

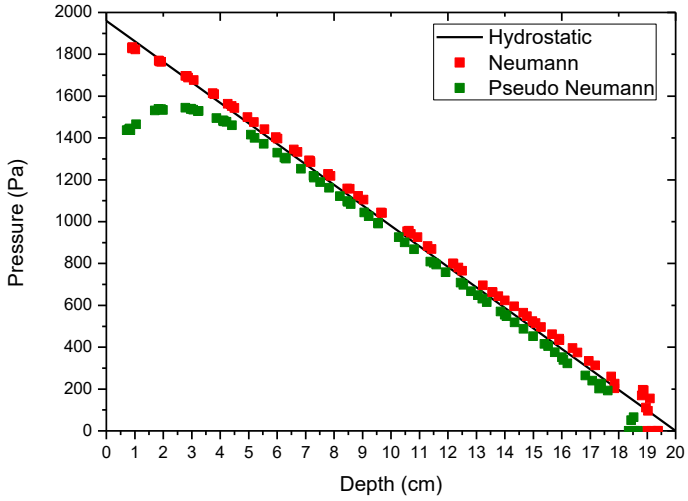

Fig. 8. Pressure distribution using different treatments and theorical hydrostatic

3.2 Dam Break Flow Validation

In this study, the experimental test used is from the investigation of dynamic pressure loads during the dam break with an opening gate, which was carried out at the Technical University of Madrid (UPM), as reported by Lobovský *et al.,* [16]. In order to validate the experiment by using the proposed scheme, the same geometry as the experimental with pressure sensors was used in the analysis model, as depicted in Figure 9. The top view and front view of the analysis model show the tank dimensions, and the initial water depth H in the dam reservoir is 600 mm with a persistent velocity of opening gates is 4.53 m s^{-1}. The chosen location of the pressure sensors used in the analysis model is the same as in the experimental, which is located in the centre-line where the second sensor (sensor 2) is placed, 15 mm above the bed and the highest sensor, which is sensor 4 located 80mm from the bottom to measure the impact of pressure.

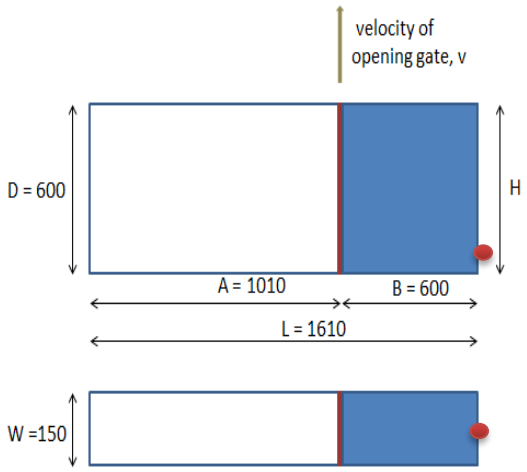

Fig. 9. Geometrical dam break problem with an opening gate [16]

The clear judgment of free surface profile evolution snapshot among the numerical simulation and the experimental at times 463.3 ±3.3ms or the dimensional time t* = 1.87, as shown in Figure 10 and Figure 11. The similarities of the deformation and snapshot on the free surface shape are detected. Then, the observation of the location of the front wavefront also shows the same tendency as the experimental one. The pressure contour in this figure indicates the pressure gradient and its impact after hitting the wall, which shows higher pressure. The results of the pressure measured at sensor 2 and sensor 4 were compared with experimental data, as shown in Figure 12 and Figure 13. The value and the arrival time of impact on the tank corner are almost similar to those in the experimental data.

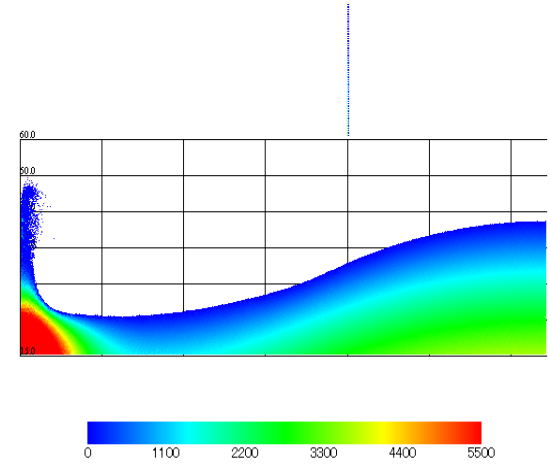

Fig. 10. Simulation results using the proposed boundary treatment at t* = 1.87

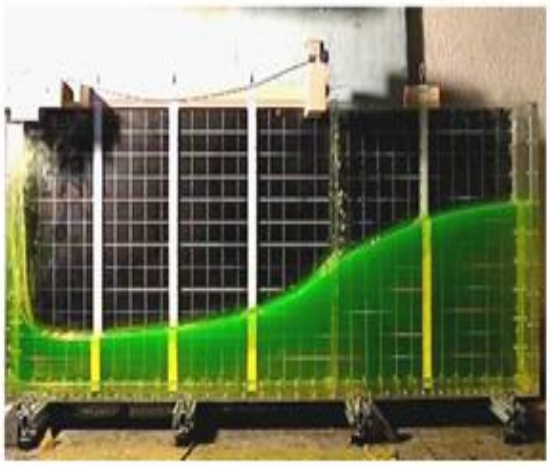

Fig. 11. Experimental results at t* = 1.87

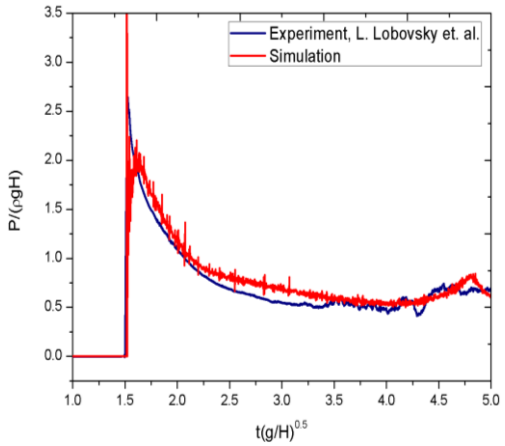

Fig. 12. Comparison of the non-dimensional pressure at sensor 2 between the simulation results and the result from the experiment

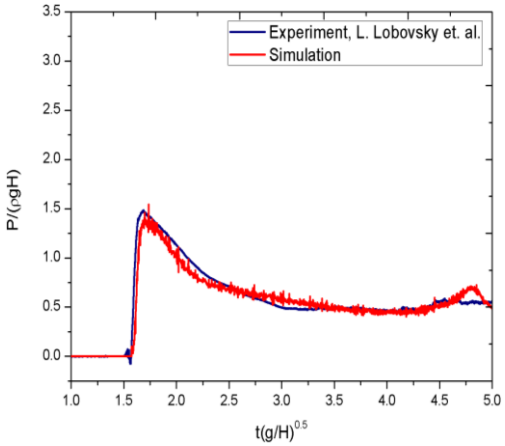

Fig. 13. Comparison of the non-dimensional pressure at sensor 4; between the experiment and simulation results

3.3 Standford Bunny Demonstration

Stanford Bunny is one of the most famous 3D-CAD objects used to demonstrate complicated irregular shapes because its 3D-CAD data can be downloaded for free. The bunny is placed at the centre of the tank, as depicted in Figure 14. The upper part of the tank consists of 0.20m of water height separated by both sides of the gates. The opening gates were moved with constant speed in both directions. This demonstration shows the applicability of the proposed boundary treatment for a dynamic motion of water within a complicated boundary.

Figure 15 presents several snapshots of the movement and pressure of the falling water and the bunny taken during the simulation at certain time stages. The snapshots illustrate the reasonable dynamic water pressure seen from the early step when the opening gate begins to operate and the water falls onto the bunny. The higher pressure is observed, especially on the top of the bunny's body and at the corner of the tank once the water falls on the bunny and hits the bottom boundary. It is apparent from these snapshots that no penetration occurred during the simulation, and the pressure reaction towards the Stanford Bunny shows a good agreement with the falling water. Furthermore,

once all the water from the top goes down, the pressure in the water domain shows the same pressure level on the bunny surface at the same depth.

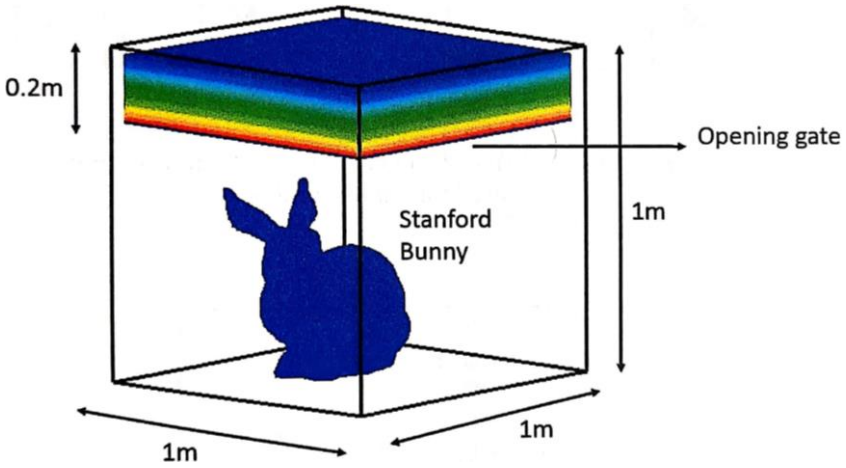

Fig. 14. Schematic diagram of Stanford Bunny used for demonstration

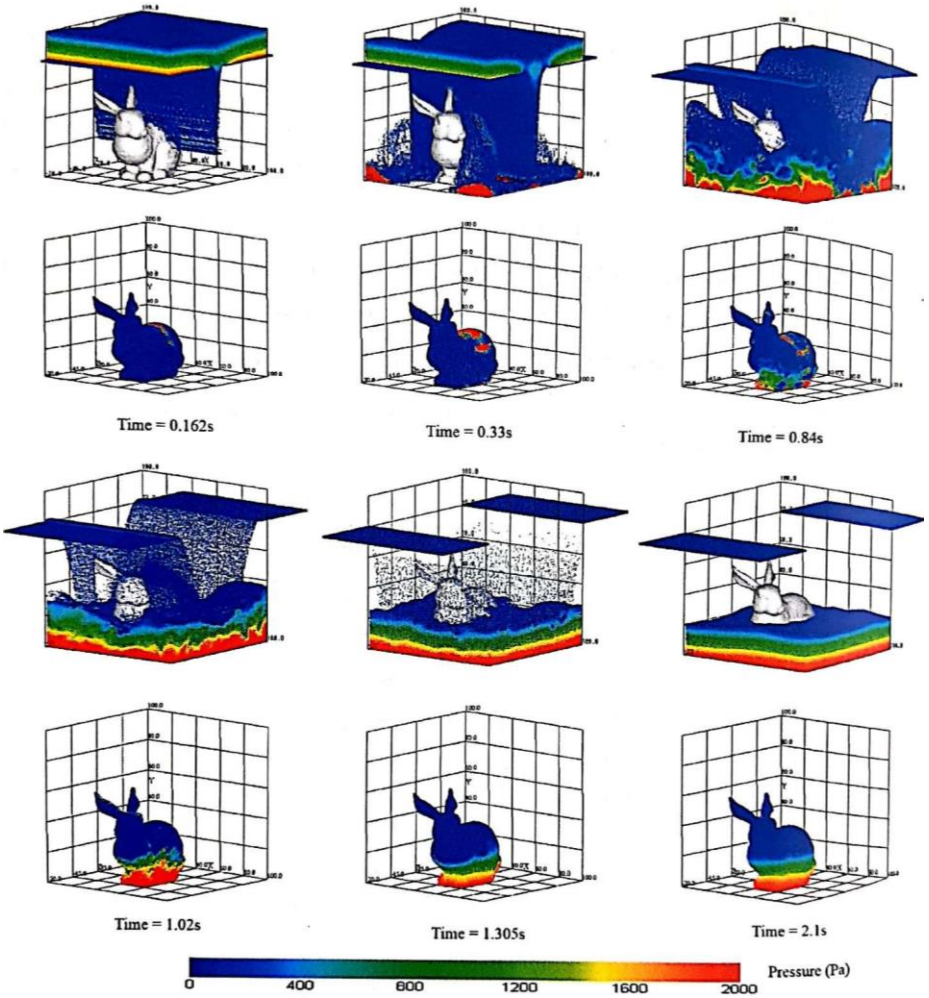

Fig. 15. Several snapshots of pressure distributions at certain times in the Stanford Bunny demonstration

4. Conclusions

Through the verification in the hydrostatic solver for the pseudo-Neumann condition and fully Neumann boundary condition that have been carried out, it was found that the fully Neumann boundary condition can simulate the accuracy and similarity to the theoretical solution with low computational costs as the CG solver used. Also, the validation test of dam break flows experimental data conducted with the proposed fully Neumann boundary condition to check the performance and the measured pressure at sensor 1 of the simulation shows good agreement with the experimental results. Another significant finding of this study is that the proposed boundary treatment produced not only a robust solution with high accuracy and low computational costs but can also be applied to a much more complicated and dynamic problem, such as the demonstration test of the Stanford Bunny model.

Acknowledgement

This research was supported by the Ministry of Higher Education (MOHE) through Fundamental Research Grant Scheme (FRGS/1/2020/TK0/UTHM/03/16) or Vot No. K315. The authors would also like to thank the Spatial Technology for Civil Engineering (STFORCE), Centre for Diploma Studies (CeDS), and Research Management Centre, Universiti Tun Hussein Onn Malaysia, for their support.

References

[1] Lucy, Leon B. "A numerical approach to the testing of the fission hypothesis." *Astronomical Journal* 82, (1977): 1013-1024. https://doi.org/10.1086/112164

[2] Gingold, Robert A., and Joseph J. Monaghan. "Smoothed particle hydrodynamics: theory and application to non-spherical stars." *Monthly Notices of the Royal Astronomical Society* 181, no. 3 (1977): 375-389. https://doi.org/10.1093/mnras/181.3.375

[3] Colagrossi, Andrea, and Maurizio Landrini. "Numerical simulation of interfacial flows by smoothed particle hydrodynamics." *Journal of Computational Physics* 191, no. 2 (2003): 448-475. https://doi.org/10.1016/S0021-9991(03)00324-3

[4] Libersky, Larry D., and Albert G. Petschek. "Smooth particle hydrodynamics with strength of materials." In *Advances in the Free-Lagrange Method Including Contributions on Adaptive Gridding and the Smooth Particle Hydrodynamics Method: Proceedings of the Next Free-Lagrange Conference Held at Jackson Lake Lodge, Moran, WY, USA 3-7 June 1990*, pp. 248-257. Berlin, Heidelberg: Springer Berlin Heidelberg, 2005. https://doi.org/10.1007/3-540-54960-9_58

[5] Morris, Joseph P., Patrick J. Fox, and Yi Zhu. "Modeling low Reynolds number incompressible flows using SPH." *Journal of Computational Physics* 136, no. 1 (1997): 214-226. https://doi.org/10.1006/jcph.1997.5776

[6] Yildiz, Mehmet, R. A. Rook, and Afzal Suleman. "SPH with the multiple boundary tangent method." *International Journal for Numerical Methods in Engineering* 77, no. 10 (2009): 1416-1438. https://doi.org/10.1002/nme.2458

[7] Marrone, Salvatore, M. A. G. D. Antuono, A. Colagrossi, G. Colicchio, D. Le Touzé, and G. Graziani. "δ-SPH model for simulating violent impact flows." *Computer Methods in Applied Mechanics and Engineering* 200, no. 13-16 (2011): 1526-1542. https://doi.org/10.1016/j.cma.2010.12.016

[8] Asai, Mitsuteru, Keisuke Fujimoto, Shoichi Tanabe, and Masuhiro Beppu. "Slip and no-slip boundary treatment for particle simulation model with incompatible step-shaped boundaries by using a virtual maker." *Transactions of the Japan Society for Computational Engineering and Science* 2013 (2013): 1.

[9] Idris, Nur' Ain, and Yoshimi Sonoda. "A multi-level tsunami run-up simulation based on 3D particle method with a virtual wave maker." *PhD diss., Kyushu University*, 2017. https://doi.org/10.15017/1807037

[10] Nguyen, Tuan Minh, Abdelraheem M. Aly, and Sang-Wook Lee. "Improved wall boundary conditions in the incompressible smoothed particle hydrodynamics method." *International Journal of Numerical Methods for Heat & Fluid Flow* 28, no. 3 (2018): 704-725. https://doi.org/10.1108/HFF-02-2017-0056

[11] Lan, Yicong, Yapei Zhang, Wenxi Tian, G. H. Su, and Suizheng Qiu. "An enhanced implicit viscosity ISPH method for simulating free-surface flow coupled with solid-liquid phase change." *Journal of Computational Physics* 474 (2023): 111809. https://doi.org/10.1016/j.jcp.2022.111809

[12] Jena, Siddharth, and Ajay Gairola. "Novel Boundary Conditions for Investigation of Environmental Wind Profile Induced due to Raised Terrains and Their Influence on Pedestrian Winds." *Journal of Advanced Research in Applied Sciences and Engineering Technology* 27, no. 1 (2022): 77-85. https://doi.org/10.37934/araset.27.1.7785

[13] Asai, Mitsuteru, Abdelraheem M. Aly, Yoshimi Sonoda, and Yuzuru Sakai. "A stabilized incompressible SPH method by relaxing the density invariance condition." *Journal of Applied Mathematics* 2012 (2012). https://doi.org/10.1155/2012/139583

[14] Cummins, Sharen J., and Murray Rudman. "An SPH projection method." *Journal of Computational Physics* 152, no. 2 (1999): 584-607. https://doi.org/10.1006/jcph.1999.6246

[15] Lee, E-S., Charles Moulinec, Rui Xu, Damien Violeau, Dominique Laurence, and Peter Stansby. "Comparisons of weakly compressible and truly incompressible algorithms for the SPH mesh free particle method." *Journal of computational Physics* 227, no. 18 (2008): 8417-8436. https://doi.org/10.1016/j.jcp.2008.06.005

[16] Lobovský, Libor, Elkin Botia-Vera, Filippo Castellana, Jordi Mas-Soler, and Antonio Souto-Iglesias. "Experimental investigation of dynamic pressure loads during dam break." *Journal of Fluids and Structures* 48 (2014): 407-434. https://doi.org/10.1016/j.jfluidstructs.2014.03.009